

PAPER • OPEN ACCESS

## Topological Data Analysis For Evaluating PDE-based Denoising Models

To cite this article: Ahmed K. Al-Jaberi and Ehsan M. Hameed 2021 *J. Phys.: Conf. Ser.* **1897** 012006

View the [article online](#) for updates and enhancements.



**IOP | ebooks™**

Bringing together innovative digital publishing with leading authors from the global scientific community.

Start exploring the collection—download the first chapter of every title for free.

# Topological Data Analysis For Evaluating PDE-based Denoising Models

Ahmed K. Al-Jaberi<sup>1</sup>, and Ehsan M. Hameed<sup>2</sup>

<sup>1</sup>Department of Mathematics, College of Education for Pure Science, University of Basrah, Basrah, Iraq.

<sup>2</sup>Department of Mathematics, College of Computer Science and Mathematics, University of Thi-Qar, Thi-Qar, Iraq.

E-mail: ahmed.shanan@uobasrah.edu.iq

**Abstract.** Image denoising is process of removing the noise (i.e. artifacts) in digital image. Noise reduction is an essential process of image processing in order to improve, analyze and interpret important information in an image. Edges are important to the visual appearance of images, to preserve important features such as edges and corners during the noise reduction process. A class of fourth- and second-order partial differential equations (PDEs) are used to optimize the trade-off between noise removal and edge preservation. Image quality assessment plays an important role in various image processing applications. It is still an active field of research. Several techniques have been suggested for measuring image quality but none of them are ideal for measuring the quality. This paper presents a new assessment of image quality based on topological data analysis (TDA) which is used for evaluating noise removal from colour images and also for assessing the performance of PDE-based denoising models. The experimental results show that the proposed assessment model gives high correlation. Furthermore, the proposed method provides very low computational load and similar extraction of characteristics to human perceptual assessment.

## 1. Introduction

Image denoising is the process of dealing a corrupt/noisy image and guessing the clean/ original image. Digital images can be noised during acquisition, compression, and transmission, so the main challenge is considered to remove noise as much as possible without eliminating the more representative properties of the image, like edges, corners, and other sharp structures. Good denoising model is to reduce noise and recover resolution loss in an image such that human visual system (HVS) is unable to detect whether the image has been denoised or not [1]. There are several benefits of using Image denoising process in different fields in terms of understanding and analyzing the images, for instance, medical image analysis, analysis of images from satellites, etc.

There are many models for handling such noise, called image filtering. Some of these filtering techniques are PDE-based denoising models which are used for removing the random noise from an image based on the information in areas surrounding the noise pixels. Therefore, assessing the quality of denoised images is not an easy task. Evaluating denoising models depend on (1) how quantity of noise in the image(s), (2) the amount of texture and structure information in the images.

In literature, many statistical approaches proposed to evaluate the outcome of denoising models such as mean squared error (MSE) [2], [3] and its logarithmic representation known as peak signal-to-noise ratio (PSNR). Where PSNR is a popular metric to measure fidelity and evaluate the quality of images, however, PSNR is not a reliable image quality measure because it is not correlating well with



perceived quality of the image by HVS [4]. This is mainly because PSNR is not considering the spatial distribution of image pixel values into consideration. For example, Figure 1 shows two different quality images while they have the same PSNR.



Figure 1: An example of two images with same PSNR [4].

A topological data analysis (TDA) approach is proposed to evaluate noise removal from colour images and also to evaluate the performance of three PDE-based image denoising models. First PDE-based denoising model is Anisotropic Diffusion (Nonlinear total variation model) [5], second model is Isotropic (Heat equation) [6], and [7] and the third one is 4<sup>th</sup>-order PDE model [8].

The rest of the paper is organised as follows. Section 2 introduces a PDE-based denoising models. Section 3 gives an overview of TDA and reasons behind suitability of topological invariants for image analysis. Experimental results will present in section 4 and end in section 5 by giving conclusion and future directions.

## 2. PDE-based denoising models

The PDE-based denoising models are introduced for noise removal, also these models could be used for decompose the image into texture and structure components. The basic idea of the denoising model is:

$$I(x, y) = u(x, y) + n(x, y),$$

where  $I(x, y)$  is the input damaged image,  $u(x, y)$  is the original (clean) image, and  $n(x, y)$  is the additive noise. Where  $I(x, y): \Omega \rightarrow \mathcal{R}^+$ , and  $u(x, y): \Omega_c \rightarrow \mathcal{R}^+$  be the functions defining the image  $\Omega$  in the RGB colour space, where  $\Omega_c \subset \Omega$ .

In [5], the problem of denoising  $I$  by taking a minimisation of image in the space of bounded variation  $BV(\mathcal{R}^2)$ . The total variation (Anisotropic diffusion) model defined in  $L^1$  is

$$\min_{u \in BV(\Omega)} \left\{ J_\lambda[I] = \int_{\Omega} |\nabla I| + \frac{\lambda}{2} \|I - u\|_{L^1} d\Omega, I = u + n \right\} \quad (1)$$

where  $\lambda > 0$  is a scaling constant (i.e. tuning parameter). The regularising term is introduced in the first part, to remove noise/ small details with observance of important features such as sharp edges and corners. while, the energy (a fidelity) term is represented in the second part. The anisotropic diffusion regularisation (TV- $L^1$ ) model is applied for noise removal from images. The minimising model is expressed by the Euler-Lagrange equation (1):

$$\begin{cases} I = u + \frac{\lambda}{2} \operatorname{div} \left( \frac{\nabla I}{|\nabla I|} \right) & \text{in } \Omega \\ \frac{\partial I}{\partial \vec{n}} = 0 & \text{on } \partial \Omega. \end{cases} \quad (2)$$

While, the formula of the total variation (Isotropic) model is defined on  $L^2$ .

$$\min_{u \in BV(\Omega)} \left\{ J_\lambda[I] = \int_{\Omega} |\nabla I|^2 + \frac{\lambda}{2} \|I - u\|_{L^2}^2 d\Omega, I = u + n \right\} \quad (3)$$

The Euler-Lagrange equation corresponding to (3) is:

$$\begin{cases} I = u + \lambda \nabla^2 I & \text{in } \Omega \\ \frac{\partial I}{\partial \vec{n}} = 0 & \text{on } \partial \Omega. \end{cases} \quad (4)$$

The finite difference method is used to solve the models TV- $L^1$  (2) and TV- $L^2$  (4) with a Dirichlet boundary condition which will output a denoised image. More information about this numerical method can be found in [7]. In future, other approximation method will be used to solve these PDE models, which introduced in [9]. The value of  $\lambda$  is chosen based on the control in noise removal and edges preservation at the same time. Therefore, difference values of  $\lambda$  are tested through applying (2) and (4) models on database of natural images. Where, Meyer. Y proves in [10] that the TV- $L^1$  model will remove the texture, if  $\lambda$  is small enough. Experimentally, the value of  $\lambda$  is 0.14 which control in noise removal and edges preservation. In addition, the 4<sup>th</sup> order model has been used to remove the noise from images. This model is proposed based on Laplacian operator, the formula of this model is:

$$\min_{u \in BV(\Omega)} \left\{ J_\lambda[I] = \int_{\Omega} f(|\nabla^2 I|) \partial \Omega \right\} \quad (5)$$

where  $\nabla^2$  denotes the Laplacian operator and  $f(\cdot) > 0$  and is an increasing function. The Euler-Lagrange equation is applied on the model (5),

$$f'(|\nabla^2 I|) \frac{\nabla^2 I}{|\nabla^2 I|} = 0 \quad (6)$$

The general details on the model (6) can be found in [8] and [11]. The gradient descent procedure has applied to the model (6):

$$\frac{\partial I}{\partial t} = -\nabla^2 \left[ f'(|\nabla^2 I|) \frac{\nabla^2 I}{|\nabla^2 I|} \right] \quad (7)$$

The finite difference method can be used to solve the model (7), more details can be found in [8] and [12]. Figure 2, below, presents the denoised images obtained from the (2), (4), and (7) models.

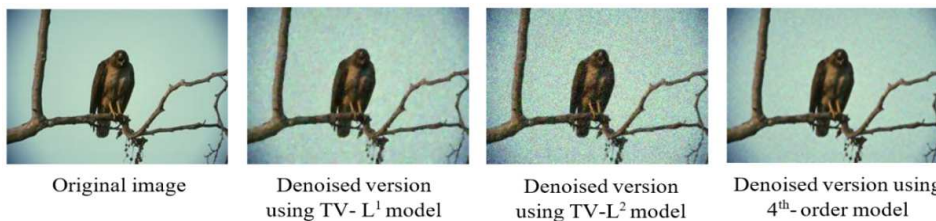


Figure 2: Comparison of three denoising models.

To sum up, the 4<sup>th</sup> order model failed to completely eliminate the noise because piecewise planar images have less masking capability than step images. On the other hand, the edges have successfully

kept in the image by using the 4<sup>th</sup> order model [8], while TV-L<sup>1</sup> and TV-L<sup>2</sup> models tend to generate multiple false edges. Moreover, the smooth denoised image generated by TV-L<sup>1</sup> is sharper than that by TV-L<sup>2</sup> [13].

### 3. Image Quality Assessment Post denoising

The aim is to study the quality evaluation of noised natural images using various PDE-based denoising models. Different types of noise have been used to check the efficacies of the 2<sup>nd</sup>- and high-order PDE-based denoising models by using TDA approach which will introduce in this section.

#### 3.1. Topological Data/Image Analysis

Topological data analysis approaches depend on reducing features from data points (objects) and then calculating pairwise similarities between them. There are several of challenges when deal with Big Data applications, as introduced in [14], [15] and [16]. Topology approaches have been used to study the closeness and connectivity properties of the object of images using a finite combinatorial operation such as Simplicial Complex (SC). There are several types of SCs, the Vietoris-Rips of SCs are used in this paper because it is easy to build and calculate in comparison with other types of SCs. The Rips SCs are built based on choosing the threshold and computing corresponding topological invariants for instance betti numbers ( $\beta_n$  for  $n = 0,1,2$ ), cliques, Euler characteristics, and others. The novel topological model uses several threshold values which that depends on the persistency of topological invariants across an increasing sequence of thresholds values is known as TDA approach.

Homology theory is used to describe the topological features. More accurately, the degree of the n-th homology group corresponds to betti numbers  $\beta_n$ , where  $\beta_0$  is represented the number of connected components (CCs),  $\beta_1$  is the number of holes and  $\beta_2$  is the number of cavities in the built Rips SC. TDA approach relies on computing the persistency of these invariants across an increasing series of thresholds using persistent homology [16] and [17]. There are many recent applications of TDA approach such as image forgery detection [18], fingerprint classification [19], brain artery [20], image tampering detection [21], image inpainting [22], gait recognition [23], steganalysis [24], classification of hepatic lesions [25], and others

The first step of constructing a SC is to select a landmark points in order to build them in higher dimensional simplices such as edges, triangles and tetrahedrons. For this purpose, we will follow the work that have been introduced by A. Asaad and S. Jassim in [26] which the use the uniform Local Binary Patterns (LBP) to select the landmark points in topological objects construction. Therefore, the next section introduces the LBP as a landmark selection procedure in the SC construction.

##### 3.1.1. Landmark point selection

LBP firstly introduced as an image texture descriptor by Ojala et al. in [27]. The idea of LBP is followed in this paper. LBP applies on the image by replaces each pixel of the image with an 8-bit binary code, which represents the texture and local structure in the image. Each pixel specifies by its 8 neighbouring pixels in a  $3 \times 3$  window surrounding it. The LBP operator works by starting from the top-left corner of the window. Then subtract the central pixel from its 8 neighbouring pixels. After that allocate 0 if the result is negative, and 1 otherwise, as seen Figure 3. The process of LBP can be mathematically written as following:

$$LBP(x_c, y_c) = \sum_{i=1}^7 \alpha(P_i - P_c)2^i \quad (8)$$

Where  $P_c$  is the center pixel value,  $P_i$  is the neighboring pixels value, and the function  $\alpha(x)$  can be written as following:

$$\alpha(x) = \begin{cases} 1 & \text{if } x \geq 0 \\ 0 & \text{if } x < 0 \end{cases} \tag{9}$$

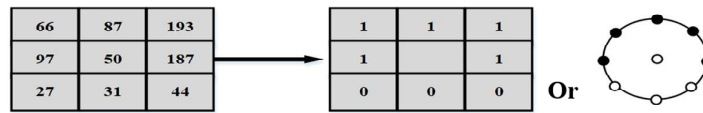


Figure 3: An example of LBP operator.

The results of applying the process of LBP on the block matrix is the binary code 11111000 (decimal = 31), as seen in Figure 3. Uniform LBP (ULBP) refers no more than 2 circular transitions in 8-bit circular bytes. The ULBP of any gray image consists of 58 unique uniform geometries. The ULBP codes represent 90% of LBP codes in the natural images [24]. Where, there are seven groups (of 8 binary codes) of ULBP according to the number of 0's and 1's in their binary codes, excepting the cases of 00000000 and 11111111. Each one of these groups represents a certain types of image textures. ULBP codes that have t consecutive 1's represent as geometry-t, such as G1, G2,..., G7. The simplicial complexes is illustrated for an original image and its 3 different denoised images as seen in Figure 4.

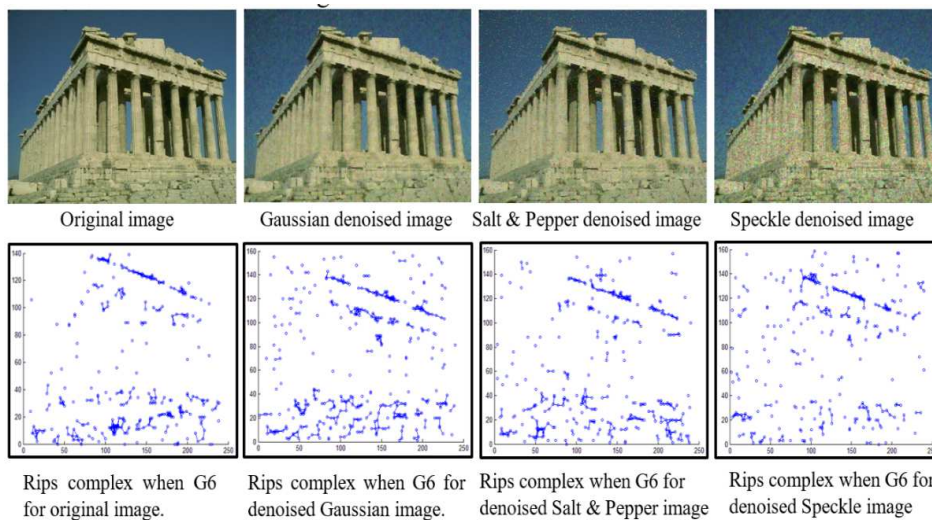


Figure 4: Sensitivity of topological invariants to denoising image.

Figure 4 is explained the SC shapes of denoised and original images are clearly different. More specific, the number of CCs counted for both the denoised and original images. The better quality of the denoised image which is the nearer number of CCs of the denoised image to the number of CCs of original image, and consequently it is the better denoising model.

### 3.1.2. Vietoris-Rips complex construction

For each class of geometry-t in ULBP are extracted in the original and its corresponding positions in forged images of the database. Then, a set of image pixel positions of the 8 sets of t-ones ULBP codes is calculated. The Euclidean distance is counted between each pairs of points in the set, and then an

increasing 8 sequence of T-dependent Rips complexes is build, one for each rotation of the geometry-t codes. 0-dimensional simplices at T=0 represents the points in the geomatry of image. Where T-threshold is gradually increased and computed  $\beta_0$  at each T. There is no optimal method to select the best threshold to captures the best topology of data sets [17]. A fixed number of distance thresholds will be used as follows:

$$T_1 = 0, T_2 = 3, T_3 = 5, T_4 = 7, T_5 = 10, T_6 = 12, T_7 = 15, T_8 = 17, T_9 = 20.$$

The fixed number of distance thresholds is used because beyond certain distance thresholds. The power of CCs number will lose its ability to discriminate denoised images from original ones. In this work, each geometry studied at different thresholds, the better threshold for assessing the quality of images is  $T = 9$ .

#### 4. Proposed Method

The procedure of building topological shapes from images are also used as an image quality assessment tool. This approach is introduced by A. Asaad and S. Jassim in [26], as they used the TDA approach to assess the quality of degraded images. Moreover, the TDA approach are applied to detect the natural forgeder images [18]. The TDA approach also has been used to improve Exemplar based inpainting method which introduced in [22]. Therefore, this section describes the use TDA proposal approach to assess the quality of image denoising and to evaluate the performance of PDE models. The diagram Figure 5 below summarises the procedures of assessing the quality of images by using TDA approach.

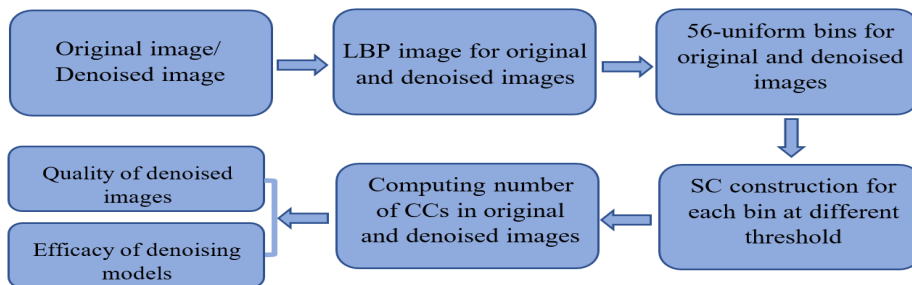


Figure 5: SCs construction for the quality of image denoising.

##### 4.1. Testing Experiments

Berkeley segmentation database [28] has used in the experiments for evaluating the convenience of the different PDE models. This database is consisted of 300 natural colour images, these images have chosen based on the quantity of texture and structure to check the efficiency of these PDE-based denoising models.



Figure 6: The same natural image with three types of noise domains.

The first two types of noise will use to check the efficacy of PDE- based denoising models in noise removal. While, the third type of noise will apply to study the ability of PDE-based denoising models to removing huge noise and to preserving edges in images. These PDE-based denoising models apply to remove the noise in each channel image and then the denoised image displays by combining of three denoised channels images. So, TDA approach will use to the assess a quality of natural denoised images and to determine the efficacy of PDE-based denoising models in the next section.

4.1.1. TDA for evaluating noise removal from colour images

After building the SCs from the bins, the obtained patterns is carefully analysed by looking at the LBP codes at different thresholdings, as a result, the cases of simplicial complexes that associated with the groups of G5 and G6 LBP codes at threshold T=9 are used to assess the quality of denoised images. The G5 and G6 groups are related with the geometric structure of a corners and an end of a line. Where these groups will play a important role as image quality assessment characteristic. After that, the number of CCs of the original images is computed and compared with three types of denoised images in 8 rotations of G5 and G6 LBP codes at T=9, as see in Figure 7.

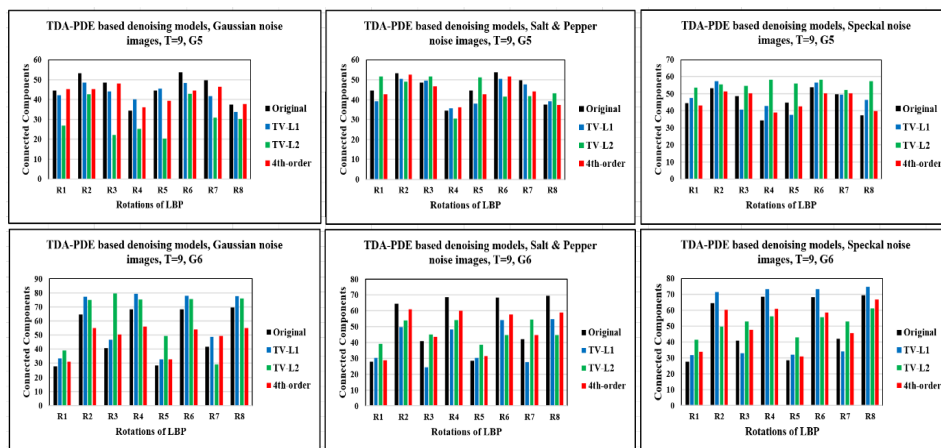


Figure 7: Quality assessment of denoised image using TDA approach at G5 and G6 in three noise types of natural dataset images.

Figure 7 showed the average of the number of CCs at 8 iterations in G5 and G6 at threshold T=9 of 3 noise types of natural dataset images that obtained using the TV-L<sup>1</sup>, TV-L<sup>2</sup> and 4<sup>th</sup>-order models. the number of CCs using the TV-L<sup>1</sup> and 4<sup>th</sup>-order models are nearer to the original images than those obtained using TV-L<sup>2</sup> model in three types of noise. More precisely, the difference is significant and more distinguishable in quality comparison between denoised images obtained using TV-L<sup>1</sup> model with those obtained using TV-L<sup>2</sup> and 4<sup>th</sup>-order models.

4.1.2. TDA for evaluating the Performance of PDE models

This section study the behaviour of PDE-based denoising models and compare their results at different iterations in three types of noise using TDA approach. These PDE-based denoising models have a finite iteration number of numerical solutions through which to remove the noise in the images. These equations are solved at different iterations to check which one of these equations rapidly arrives at a steady state to remove the noise in the images, as seen in Figure 8, 10, and 12. The denoised images using three PDEs show in each row of these figures at a certain iteration and so on for other

rows. Figure 9, 11, and 13 display the average of the numbers of CCs in the original and denoised images at threshold  $T=9$  in G5.

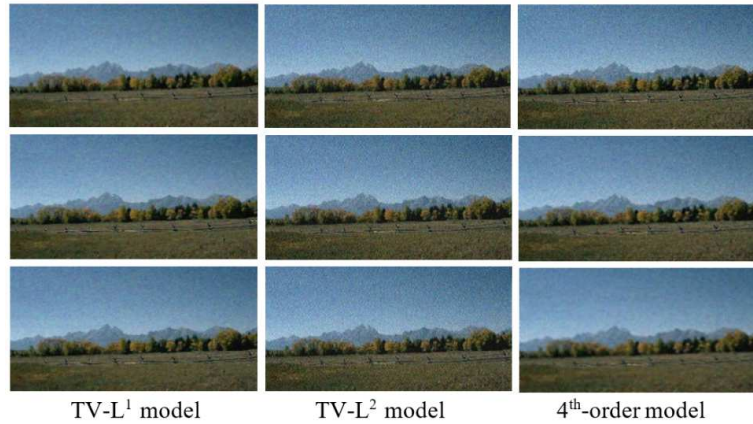


Figure 8: Gaussian noise removal using PDE-based denoising models. Row 1, Row 2, and Row 3 denoised images using three models at 50, 100, and 200 iterations, respectively.

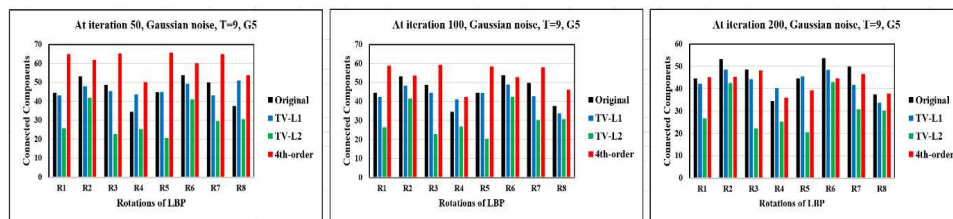


Figure 9: Evaluation of performance of PDE-based denoising models using TDA approach at different iterations for denoising Gaussian noise in G5 at threshold  $T=9$ .

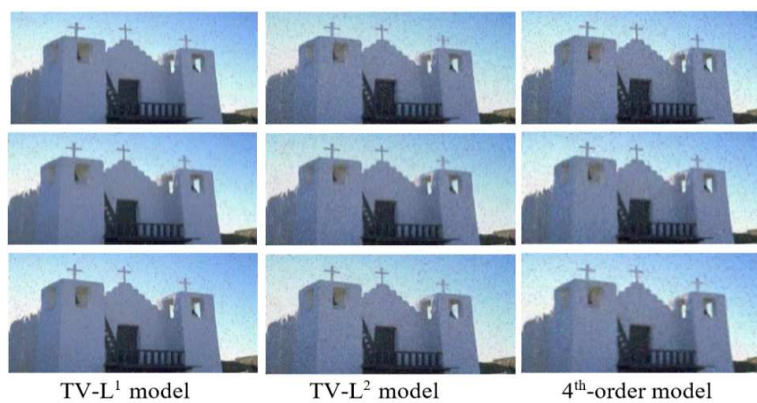


Figure 10: Salt & Pepper noise removal using PDE-based denoising models. Row 1, Row 2, and Row 3 denoised images using three models at 50, 150, and 300 iterations, respectively.

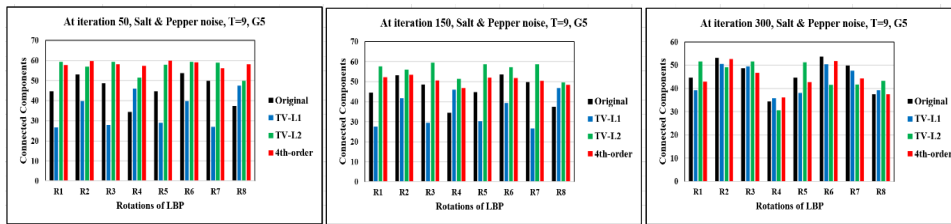


Figure 11: Evaluation of performance of PDE-based denoising models using TDA approach at different iterations for denoising Salt and Pepper noise in G5 at threshold  $T=9$ .

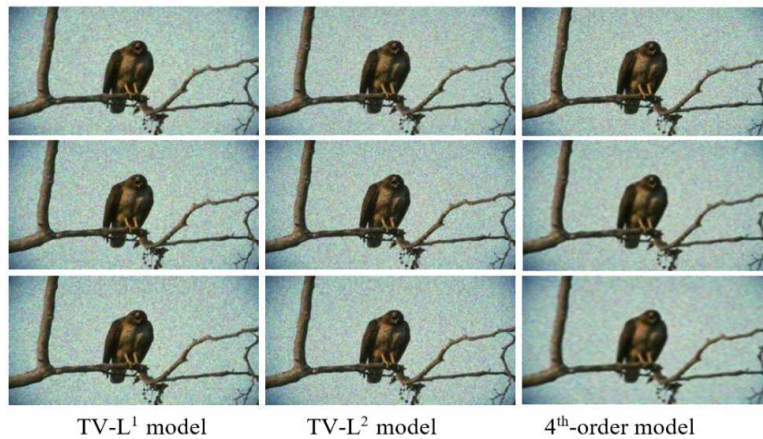


Figure 12: Speckle noise removal using PDE-based denoising models. Row 1, Row 2, and Row 3 denoised images using three models at 100, 250, and 500 iterations, respectively.

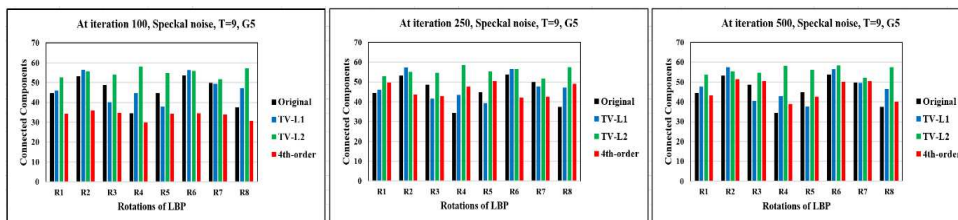


Figure 13: Evaluation of performance of PDE-based denoising models using TDA approach at different iterations for denoising Speckle noise in G5 at threshold  $T=9$ .

The TV- $L^1$  and TV- $L^2$  models need large numbers of iterations to arrive in a steady state while the 4<sup>th</sup>-order model need small number of iterations to arrive in a steady state because it use more information in the boundary conditions. Moreover, the TV- $L^1$  and TV- $L^2$  models are consumed a less time to arrive in the steady state than in the 4<sup>th</sup>-order model because the TV- $L^1$  and TV- $L^2$  models are of 2<sup>nd</sup> order.

**5. Conclusion and future works**

TDA approach proposed to assess the quality of natural denoised images and to study the efficacy of PDE-based denoised models. More accurately, the number of CCs is counted for both the denoised

and original images. The closer number of CCs of the denoised image to the number of CCs of original image, is the better quality of the denoised image, and consequently is the better denoising model. Experimental results showed the efficacies of TV-L<sup>1</sup> and 4<sup>th</sup>-order model for removing the noise is better than TV-L<sup>2</sup> model, and the efficacies of 4<sup>th</sup>-order model in edges preservation is better than TV-L<sup>1</sup> and TV-L<sup>2</sup> models. Also, the TV-L<sup>1</sup> and TV-L<sup>2</sup> models needed large number of iterations to arrive in the steady state however they are still faster than in the 4<sup>th</sup>-order model. The TDA approach gave a good evaluation of image denoising quality because their results corresponding with their qualitative results. In future, other types of noise and denoising models will be used to extend this investigation, and consequently analysis the quality of images under these effects.

## References

- [1] H. R. S. & A. C. Bovik, 2006, *Image information and visual quality*, (IEEE Journals & Magazine). [Online]. Available: <https://ieeexplore.ieee.org/abstract/document/1576816>.
- [2] D. M. Chandler, 2013, *Seven Challenges in Image Quality Assessment: Past, Present, and Future Research*, (International Scholarly Research Notices). [Online]. Available: <https://new.hindawi.com/journals/isrn/2013/905685/>.
- [3] P. Mohammadi, A. Ebrahimi-Moghadam, and S. Shirani, 2014, *Subjective and Objective Quality Assessment of Image: A Survey*, *arXiv Prepr. arXiv1406.7799*.
- [4] S. Winkler and P. Mohandas, 2008, *The Evolution of Video Quality Measurement: From PSNR to Hybrid Metrics*, (IEEE Trans. Broadcast), vol. 54, no. 3, pp. 660–668.
- [5] L. I. Rudin, S. Osher, and E. Fatemi, 1992, *Nonlinear total variation based noise removal algorithms*, (Phys. D Nonlinear Phenom), vol. 60, no. 1–4, pp. 259–268.
- [6] J. Weickert, 1996, *Theoretical Foundations of Anisotropic Diffusion in Image Processing*, pp. 221–236.
- [7] L. A. Vese and S. J. Osher, 2003, *Modeling Textures with Total Variation Minimization and Oscillating Patterns in Image Processing*, (J. Sci. Comput), vol. 19, no. 1/3, pp. 553–572.
- [8] Y. L. You and M. Kaveh, 2000, *Fourth-order partial differential equations for noise removal*, (IEEE Trans. Image Process), vol. 9, no. 10, pp. 1723–1730.
- [9] M. Ahmed K. Al-JABERI.1 , Ehsan M. HAMEED.2, 2020, *A Novel Analytic Method For Solving Linear And Non-Linear Telegraph Equation*, (PERIÓDICO TCHÊ QUÍMICA), vol. 17, no. 35, pp. 536-548.
- [10] Y. Meyer, 2002, *Oscillating Patterns in Image Processing and Nonlinear Evolution Equations*, (University Lecture Series), Vol. 22, Amer. Math. Soc..
- [11] H. Strobel, Strang, G., 1989, *Introduction to Applied Mathematics*. Wellesley, Mass. Wellesley-Cambridge Press 1986. IX, 758 pp. ISBN 0-9614088-0-4,” (ZAMM - J. Appl. Math. Mech. / Zeitschrift für Angew. Math. und Mech)., vol. 69, no. 9, pp. 311–312.
- [12] A. L. Bertozzi and A. L. Bertozzi, 1998, *The Mathematics of Moving Contact Lines in Thin Liquid Films*.
- [13] Jiyiing Wu and Qiuqi Ruan, 2008, *A novel hybrid image inpainting model*, (in 2008 International Conference on Audio, Language and Image Processing), pp. 138–142.
- [14] G. Carlsson, 2009, *Topology And Data*, (Bull. New. Ser. Am. Math. Soc), vol. 46, no. 209, pp. 255–308.
- [15] P. Y. Lum *et al.*, 2013, *Extracting insights from the shape of complex data using topology*, *Sci. Rep.*, vol. 3, no. 1, p. 1236.
- [16] H. Edelsbrunner, 2012, *Persistent Homology: Theory And Practice*, (Ernest Orlando Lawrence Berkeley Natl. Lab. Berkeley), CA, vol. LBNL-6037E.
- [17] R. Ghrist, 2008, *Barcodes: The persistent topology of data*, (in Bulletin of the American

- Mathematical Society), vol. 45, no. 1, pp. 61–75.
- [18] A. K. Al-Jaberi, A. Asaad, S. A. Jassim, and N. Al-Jawad, 2020, *Topological Data Analysis for Image Forgery Detection*, (Indian Journal of Forensic Medicine & Toxicology), vol. 14, no. 3, pp. 1745-1751.
  - [19] N. Giansiracusa, R. Giansiracusa, and C. Moon, 2017, *Persistent homology machine learning for fingerprint classification*.
  - [20] P. Bendich, J. S. Marron, E. Miller, A. Pieloch, and S. Skwerer, 2016, *Persistent Homology Analysis of Brain Artery Trees*, (Ann. Appl. Stat), vol. 10, no. 1, pp. 198–218.
  - [21] A. Asaad and S. Jassim, 2017, *Topological Data Analysis for Image Tampering Detection*, (Springer, Cham), pp. 136–146.
  - [22] S. A. Jassim, A. Al-jaberi, A. T. Asaad, and N. Al-Jawad, 2018, *Topological data analysis to improve exemplar-based inpainting*, (in Mobile Multimedia/Image Processing, Security, and Applications 2018), vol. 10668, p. 4.
  - [23] J. Lamar-León, E. B. García-Reyes, and R. Gonzalez-Diaz, 2012, *Human Gait Identification Using Persistent Homology*, (Springer, Berlin, Heidelberg), pp. 244–251.
  - [24] T. Ahonen, A. Hadid, and M. Pietikainen, 2006, *Face Description with Local Binary Patterns: Application to Face Recognition*, (IEEE Trans. Pattern Anal. Mach. Intell), vol. 28, no. 12, pp. 2037–2041.
  - [25] A. Adcock, D. Rubin, and G. Carlsson, 2014, *Classification of hepatic lesions using the matching metric*, (Comput. Vis. Image Underst), vol. 121, pp. 36–42.
  - [26] A. T. Asaad, R. D. Rashid, and S. A. Jassim, 2017, *Topological image texture analysis for quality assessment*, vol. 10221, p. 102210I.
  - [27] T. Ojala, M. Pietikäinen, and D. Harwood, 1996, *A comparative study of texture measures with classification based on featured distributions*, (Pattern Recognit.), vol. 29, no. 1, pp. 51–59.
  - [28] C. F. and D. M. Pablo Arbelaez, 2007, *The Berkeley Segmentation Dataset and Benchmark*.